REPORT DOCUMENTATION PAGE

Form Approved

OMB No. 0704-0188

1. AGENCY USE ONLY (Leave Blank)	2. REPORT DATE	3. REPORT TYPE AND DATES COVERED
	3 September 2003	Final (12/1/02 – 11/30/06)

4. TITLE AND SUBTITLE

Mid-to-High-Frequency Bottom Loss in the East China Sea

5. FUNDING NUMBERS

N00014-03-1-0271

6. AUTHOR(S)

Jee Woong Choi and Peter H. Dahl

7. PERFORMING ORGANIZATION NAME(S) AND ADDRESS(ES)

Applied Physics Laboratory
University of Washington
1013 NE 40th St.
Seattle, WA 98105-6698

8. PERFORMING ORGANIZATION REPORT NUMBER

9. SPONSORING/MONITORING AGENCY NAME(S) AND ADDRESS(ES)

Office of Naval Research
One Liberty Center
875 North Randolph St., Ste. 1425
Arlington, VA 22203-1995
Attn: Dr. Ellen S. Livingston, Code 0321

10. SPONSORING/MONITORING AGENCY REPORT NUMBER

11. SUPPLEMENTARY NOTES

12a. DISTRIBUTION/AVAILABILITY STATEMENT

Approved for public release

DISTRIBUTION STATEMENT A
Approved for Public Release
Distribution Unlimited

12b. DISTRIBUTION CODE

13. ABSTRACT (Maximum 200 words)

Bottom loss measurements made in the East China Sea in 2001 as part of the Asian Sea International Acoustics Experiment as a function of frequency (2–20 kHz) and seabed grazing angle (15°–24°) are presented. The measurements are interpreted as estimates of the modulus of the plane wave reflection coefficient, and data are compared to predictions using a reflection coefficient model, based on a two-layered sediment for which sound speed in the surficial sediment layer is allowed to vary as a linear k^2 profile, where k is acoustic wave number. The region below this layer is modeled as a half-space with constant density and sound speed. The reflection coefficient model is driven by eight geoacoustic parameters. This parameter set produced model curves that agreed reasonably well with observations of bottom loss over the entire frequency range. Since this data set does not provide detailed information about sediment structure for depths beyond about 3 m, the geoacoustic parameter set is more properly viewed as description of the sediment layer and sediments in the underlying 2 m. Similarly, a self-consistent construction of a geoacoustic model for the East China Sea should necessarily amalgamate the mid to high frequency results given here with results obtained at lower frequencies.

14. SUBJECT TERMS

Bottom loss, bottom reflection, geoacoustic parameters, ocean acoustic propagation, sediment layering

15. NUMBER OF PAGES

8

16. PRICE CODE

17. SECURITY CLASSIFICATION OF REPORT	18. SECURITY CLASSIFICATION OF THIS PAGE	19. SECURITY CLASSIFICATION OF ABSTRACT	20. LIMITATION OF ABSTRACT
Unclassified	Unclassified	Unclassified	UL

Mid-to-High-Frequency Bottom Loss in the East China Sea

Jee Woong Choi and Peter H. Dahl

Abstract—**Bottom-loss measurements made in the East China Sea in May–June 2001 as part of the Asian Sea International Acoustics Experiment as a function of frequency (2–20 kHz) and seabed grazing angle (15°–24°) are presented. The measurements are interpreted as estimates of the modulus of the plane wave reflection coefficient and data are compared to predicted values using a reflection coefficient model, based on a two-layered sediment for which the sound speed in the surficial sediment layer is allowed to vary as a linear k^2 profile, where k is acoustic wave number. The region below this layer is modeled as a half-space with constant density and sound speed. The reflection coefficient model is driven by eight geoacoustic parameters; these are estimated from the data by minimizing the weighted squared error between the data and the model predictions for a candidate set of parameters. The parameter estimates for the sediment layer are thickness, 0.9 ± 0.5 m; density, 2.0 ± 0.1 g/cm^3; and attenuation, 0.25 ± 0.05 dB/m/kHz, with sediment layer sound speed increasing from 1557 ± 4 m/s at the water–sediment interface to 1625 ± 35 m/s at a depth of 0.9 m. The parameter estimates for the half-space are density, 2.0 ± 0.1 g/cm^3; attenuation, 0.25 ± 0.15 dB/m/kHz; and sound speed, 1635 ± 52 m/s. Variances for these estimates are derived using the Bootstrap method. This parameter set produced model curves that agreed reasonably well with the observations of bottom loss over the entire frequency range and is consistent with the range of independently measured geoacoustic variables. Since this mid-to-high-frequency data set does not provide detailed information about the sediment structure for depths beyond about 3 m, the geoacoustic parameter set is more properly viewed as description of the sediment layer and sediments in the underlying 2 m. Similarly, a self-consistent construction of a geoacoustic model for the East China Sea should necessarily amalgamate the mid-to-high-frequency results given here with results obtained at lower frequencies.**

Index Terms—**Bottom loss, bottom reflection, geoacoustic parameters, ocean acoustic propagation, sediment layering.**

I. Introduction

THIS paper presents results of an experiment to measure the modulus of the mid-to-high-frequency bottom reflection coefficient, via bottom-loss measurements, at one site in the East China Sea as part of the 2001 Asian Seas International Acoustics Experiment (ASIAEX). The measurements were conducted 350 km east of Shanghai, China, in the Chinese continental margin (Fig. 1), at location 29° 39'N, 126° 49'E in waters 105 m in depth, in an area historically characterized by very fine sand sediment [1].

Manuscript received June 11, 2003; revised September 3, 2003. This work was supported by the Office of Naval Research under Code 321 Ocean Acoustics.

The authors are with the Applied Physics Laboratory, University of Washington, Seattle, WA 98105-6698 USA (e-mail: choijw@apl.washington.edu; dahl@apl.washington.edu).

Digital Object Identifier 10.1109/JOE.2004.834178

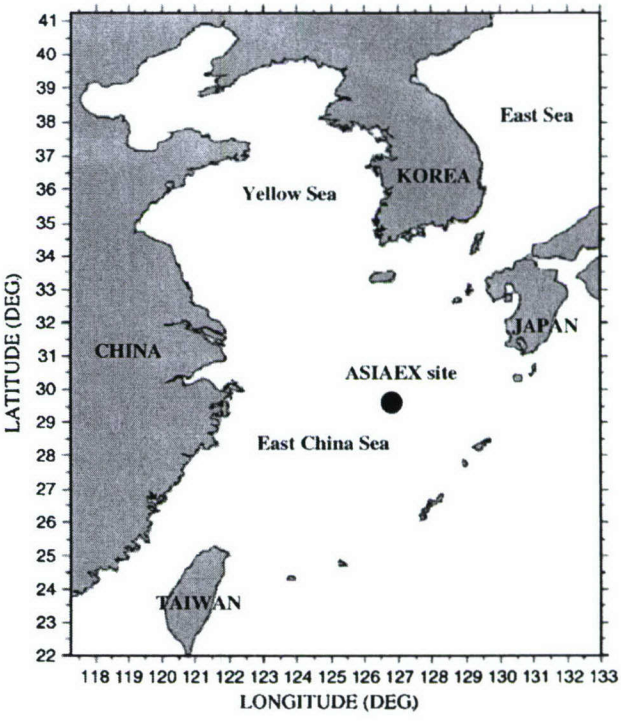

Fig. 1. Location of the ASIAEX East China Sea experimental site. The measurements were made within O (100) m of the position 29° 39'N, 126° 49'E; water depth is 105 m.

Data were collected as function of frequency (range 2–20 kHz) and grazing angle (range 15°–24°) and the observable is an estimate of bottom loss based on averaged intensity. This observable is compared to $-20 \log |R|$, where $|R|$ is the modulus of the plane wave reflection coefficient. The range of grazing angle, though limited, was designed to span the expected critical angle, which is a key factor influencing sound propagation in a shallow-water waveguide and a point about which $|R|$ will show stronger variation with grazing angle. Observations are compared to predictions for which the forward problem consists of computing $|R|$ associated with a two-layered sediment underlying a water layer, based on candidate sets of geoacoustic parameters. An optimum set of geoacoustic model parameters is identified from an exhaustive search over a constrained parameter space based on a weighted least-squared error criterion.

Geoacoustic ground truth measurements of the experimental site were made in 2000 and 2001 as part of the ASIAEX East China Sea field program. These are in the form of gravity and piston cores and water-gun and chirp sonar generated subbottom

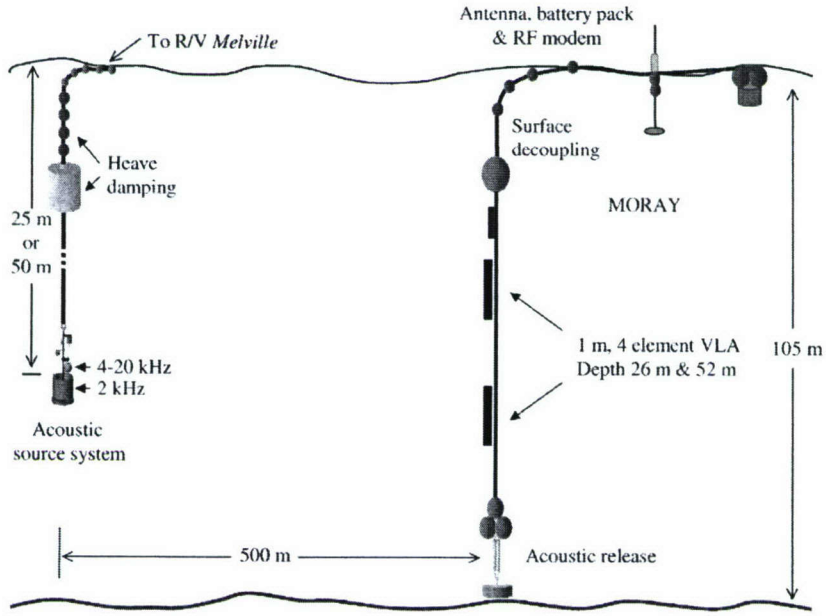

Fig. 2. Acoustic source system (left) and receiving vertical line array system (right) used to measure bottom loss. The data presented in this paper are from a single hydrophone from each of the two vertical line arrays.

profiles (see Miller *et al.* [1] for detailed discussion of geoacoustic measurements). In short, these data suggest a subbottom structure at the ASIAEX site that consists of a layer of sediment of variable thickness starting at the water–sediment interface, for which near the site of acoustic measurements the thickness was of O (1 m). Coring data [1] obtained within 100 m of the site of acoustic measurements indicate a sound speed going from approximately 1575 m/s at the water–sediment interface to 1600–1675 m/s at approximately 1 m into the sediment. There is also evidence of centimeter-scale layering superimposed on this gradual increase. The coring data also show a mean grain size (in phi scale) of 3.47ϕ, consistent with very fine sand, and bulk density between 1.85–2.05 g/cm^3. The root mean square (rms) bottom relief was 0.005 m within a 4-m measurement aperture based on the measurements of fine-scale bottom properties by Tang [2], made at the precise location of the acoustic bottom loss measurements reported here.

This paper is organized as follows. The field-measurement procedure and estimation of bottom loss are described in Section II and results are presented in Section III. Section IV outlines the bottom-reflection model based on a two-layered fluid sediment for which a sediment layer with positive sound speed gradient is sandwiched between sea water and a homogeneous half-space. This model is used in forward calculations of the reflection coefficient, which in turn are used in Section V in an exhaustive search for geoacoustic parameters that minimize error between modeled and measured bottom loss. A summary and the conclusion are given in Section VI.

II. Field Measurments and Estimation of Bottom Loss

Bottom-reflection loss measurements were made on May 31 and June 5, 2001 and were part of set of nominally 0.5-km range propagation measurements designed to study both sea surface and seabed scattering and reflection. Some results pertaining to the sea surface are discussed in [3]. An acoustic source system was deployed off the stern of the R/V *Melville* (while it maintained dynamic positioning) at a depth of either 25 or 50 m. A family of five transmit waveforms, CW pulses with a length of 2 or 3 ms and center frequency equal to 2, 4, 8, 16, and 20 kHz, plus two additional waveforms, was cycled every 100 s for 20 times; data corresponding to a set of 20×7 transmissions was identified as an experimental set, with this process repeated after a few seconds delay. An ITC 2010 transducer from International Transducer Corporation, Santa Barbara, CA, was used for the 2-kHz transmission and an ITC (omnidirectional) 1007 transducer was used for all other transmissions. At 2 kHz, the transmit pattern for the ITC 2010 used in this study is invariable within the vertical angular range 0°–20° and there is approximately a 0.5-dB change between 20°–25° at most. Thus, both transmitting systems are considered to be omnidirectional over the angular range used in the measurements. The transmissions were received on two colocated vertical line arrays, each of length 1 m, with one array at depth 26 m and the other array at depth 52 m, referenced to the array center (Fig. 2). The two-array system, called moored receiving array (MORAY), was deployed at a nominal range of 500 m from the source with precise range depending on measurement time and established acoustically. Data for this analysis originate from single omnidirectional elements (ITC 1042) on the 26- and 52-m-depth receiving array. The data were sampled at 50 kHz and sent back to the *Melville* through a radio-frequency (RF) modem.

Sound speed profiles were monitored with frequent conductivity-temperature-depth (CTD) casts made from both the *Melville* and the nearby Chinese R/V *Shi Yan 3*. In general, the sound speed versus depth variation in the East China Sea is linked to the tides during the late spring and summer months, and the sound speed in the upper mixed layer (nominal depth

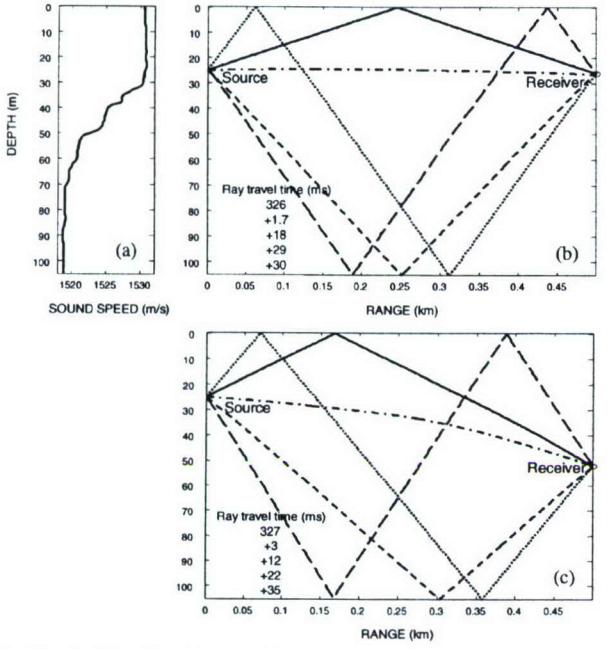

Fig. 3. (a) First five eigenrays based on the sound speed profile for set 10. Source depth and range between source and receiver are 25 and 499 m, respectively. (b) Receiver depths 26 m for the upper array and (c) 52 m for the lower array.

30 m) often varied between 1525–1530 m/s, while the sound speed near the water–sediment interface was a stable 1519 m/s.

Fig. 3 shows propagation conditions for measurement set 10, obtained at 1030 UTC May 31, and for which the source depth was set to 25 m; (a) shows the sound speed profile; (b) and (c) show eigenrays corresponding to the first five arrivals (direct, surface, bottom, surface–bottom, and bottom–surface), based on the sound speed profile in (a) and computed using a generic ray-based propagation code. The upper and lower receiving arrays each sample slightly different bottom bounce grazing angles, in this case 18.1° for the upper array and 15.3° for the lower array. A range of bottom-grazing angles between 15°–21° was achieved through using the combination of upper and lower receiving arrays, the two source depths at 25 and 50 m, plus variation in source to receiver range over the course of the experiment that was between 400–500 m. Finally, this grazing angle range was extended to 24° by exploiting data that involved a single sea-surface interacting path in addition to a bottom bounce path. Clearly, coherent reflection from the sea surface, for which the rms wave height varied but was never below about 0.2 m, was negligible. Instead, intensity is all incoherent; sea-surface interaction imparts no energy loss provided all intensity, which undergoes both time and angle spreading, is measured. This criterion is satisfied with our wide-beam widths and receive time window. Energy loss associated with attenuation from near surface bubbles can occur, but this effect is negligible under experimental field conditions sampled for these measurements characterized by mild wind speed (less than about 5 m/s) [4], [5]. Thus, in these cases the measured loss in bottom-interacting paths in excess of that due to chemical absorption and geometric spreading (both of which must be modeled), is taken to be associated with the bottom loss. The bottom-loss estimates at

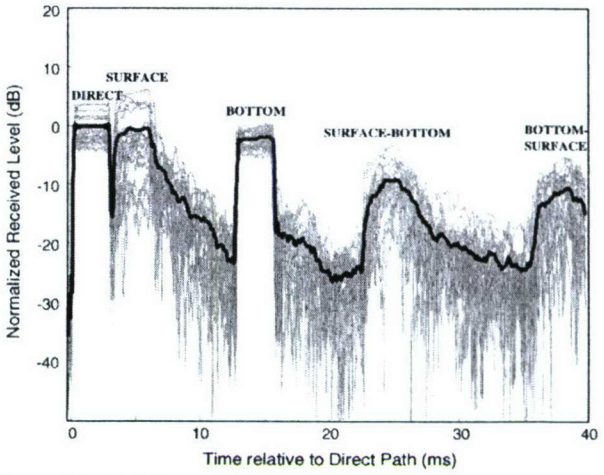

Fig. 4. Individual pings (thin lines) and average intensity based on a 20-ping average (thick line) of 16-kHz data for the lower receiver array for set 10.

grazing angles greater than 21°, however, are encumbered with a higher variance owing to fluctuations imparted by interaction with the sea surface.

Fig. 4 shows the received intensity level for 20 individual pings (thin lines) and their average intensity (thick line) for the 16-kHz measurements received on the lower receiver array for set 10. The intensity level is referenced to that of the mean peak level for the direct path, which here is assigned (arbitrarily in this figure) to be 0 dB. The ray-based spreading and absorption loss estimate for the direct path is 57.1 dB and that for the bottom bounce path is 54.7 dB. In this case, the direct path has slightly higher spreading loss owing to refraction in the water column. Absorption loss was predicted with [6] using salinity and temperature measured by CTD. These values, in combination with the mean level for the bottom-interacting path, -2.5 dB, give an estimate for $-20\log|R|$ equal to 4.9 dB at 15° for 16 kHz. However, a total energy measure, based on an integral over a time window somewhat greater than the pulse length, is used to bottom loss in the manner of [7]. This estimate puts $-20\log_{10}|R|$ equal to 4.4 dB, which becomes our reported estimate. Statistical fluctuations in the level of the single bottom-reflected path based on 20-ping average are ± 1.4 dB, which are added in quadrature to the estimated error for source level, ± 0.9 dB, giving a total uncertainty for this estimate as ± 1.7 dB. Note that total measurement uncertainty varied depending on measurement time of day and frequency. For grazing angles for estimates involving the sea-surface bounce path, total uncertainty was dominated by statistical fluctuations, which put this value closer to ± 3 dB. Finally, the total energy measure is essential for data that involved a single sea-surface interacting path because of time spread. In this case, the length of time window must be wide enough to contain the effect of time spreading of the acoustic signal caused by sea surface roughness.

For the single bottom-reflection path, minimal pulse elongation is observed, owing that we believe to the bottom boundary being acoustically smooth, as evidenced by Tang's [2] estimate for rms seabed relief H being 0.005 m. A measure of roughness is the Rayleigh parameter $\chi = 2\,kH\sin(\theta_g)$, where k is acoustic wave number and θ_g is the nominal grazing angle.

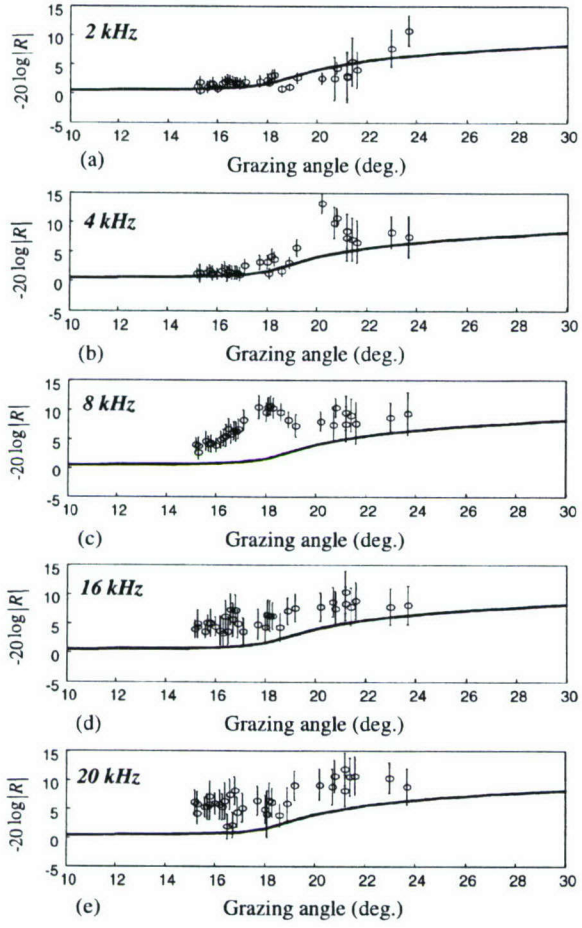

Fig. 5. Measured bottom loss as a function of grazing angle and frequency compared to model for $-20 \log |R|$ based on a homogenous half-space representation for the seabed.

At 16 kHz and grazing angle 15.3° $\chi = 0.18$ and in general $\chi \leq 0.34$ for all measurements based on the highest frequency and grazing angle, 20 kHz and 24°, respectively, indicating that the bottom is an acoustically flat surface and the reflected field is primarily generated within the first Fresnel zone [8], [9]. At 2 kHz, the first Fresnel zone for the single bottom-reflected signal for the upper receiver for set 10 is an approximate ellipse 61 m × 19 m and at 20 kHz this ellipse is reduced to 19 m × 6 m; for the lower receiver, the Fresnel zone is slightly larger. The Fresnel zone dimensions for the surface–bottom path are of the same order. Thus, these measurements represent an inherent range average over ranges of order 10–100 m.

III. Measurement Results

Fig. 5 shows estimates of bottom loss expressed in decibels as a function of grazing angle and frequency and assumed to correspond to $-20 \log |R|$. Measurements for which the grazing angle is greater than 21° are based on paths that interacted once with the sea surface and have greater uncertainty owing to fluctuations imparted by interaction with the sea surface. Measurement variance at all grazing angles tends to increase with frequency. The scintillation index (normalized variance of intensity) for the bottom reflected path generally goes from about 0.01 to 0.2 for the frequency range 2–20 kHz, increasing roughly linearly with frequency. Therefore, we assume that the increasing spread of measured data with frequency is associated with fluctuations linked to small-scale sound speed changes in the water column. Other sources of variation in the data are postulated to be associated with the existence of finer (centimeter-scale) layering and scattering from volume inhomogeneities within the sediment; however, further study of these effects is beyond the scope of this paper.

It is of interest, and useful for reference, to first compare our measurements to a homogeneous fluid half-space model for $-20 \log |R|$, as shown by the curves in Fig. 5. The density, sound speed, and attenuation coefficient for this model are 1.78 g/cm^3, 1600 m/s, and 0.15 dB/m/kHz, respectively. These geoacoustic parameters were estimated by Tang [10] using ambient noise within the 1–3-kHz band recorded on a vertical line array that was also deployed from the R/V *Melville*. The half-space model clearly does not predict the variation as a function of grazing angle seen in the measurements at frequencies greater than 2 kHz. Still, the half-space model does reasonably well in predicting the 2-kHz data (with the exception of the two measurements made at grazing angles greater than 22°).

In the next section, sediment layering will be considered as the cause of frequency and angle dependence in estimates of bottom loss, and a layer will be incorporated into a forward model for the seabed reflection coefficient. Holland [11] has also reported similar angular dependence in bottom-loss measurements over this frequency range, his measurements illustrating an influence of fine-scale layering on reflection.

IV. Forward Model for the Bottom-Reflection Coefficient

As noted previously, the subbottom structure in the East China Sea is considered, according to the findings of Miller *et al.* [1], to have an O (1-m) thick layer of sediment starting at the water–sediment interface at the experimental site. Given this finding, we postulate a forward model for the reflection coefficient to consist of a water layer overlying a two-layered fluid sediment. This can be expressed as [8]

$$R = \frac{R_{12}(1 + R_{23}) + R_{23}(1 + R_{21})}{1 - R_{21}R_{23}} \tag{1}$$

where R_{ij} is the reflection coefficient at boundary ij and subscripts 1–3 indicate water, finite-depth layer, and half-space, respectively. Additional specifications of the forward model are as follows. Layer 2 (or the sediment layer), of thickness L, is allowed to have some positive sound speed gradient, consistent with the existence of sandy sediments [12]. Layer 3 is modeled as an infinite half-space of constant sound speed that terminates the bottom impedance. Given the 2–20-kHz frequency range and $\leq 25°$ grazing angle range, moderate sediment attenuation renders our measurements insensitive to sediment properties greater than a few meters in depth; therefore, as a practical matter, our inversion goal is to identify a starting sound speed for layer 3. In other words, we have no information in our acoustic data to justify additional details in layer 3, e.g., such

as additional layered structure and sound speed gradients, etc. The *a priori* information that the sediment thickness L is O (1 m), puts $kL \geq 8$ for the lowest frequency of 2 kHz. Robins [13] suggests that density gradients have decreasing influence on bottom loss for this condition. Thus, the density in layer 2 is assumed to be some constant value, with same assumption for the density in layer 3 (but it is allowed to differ from that in layer 2). Finally, constant values (but not necessarily the same) for sediment attenuation are assigned to layers 2 and 3, and sediment attenuation is included by making the sound speed complex in the manner of [14]. We believe that such a model for the bottom-reflection coefficient roughly matches the inherent resolving capability of the measurements. For example, looking ahead to the next section, measurements made at 4 and 8 kHz clearly exhibit oscillations as a function of grazing angle that can only be reconciled with a model that includes some kind of layered structure in the upper sediments.

The model of Ainslie [15] (see also [16]) accommodates the previous formulation for the plane wave reflection coefficient by providing analytical solutions of the depth-dependent Helmholtz equation for certain canonical gradients. Elements of this model are laid out as follows. The boundary condition that the pressure and normal component of particle velocity are continuous across a boundary is imposed to obtain the reflection coefficient for each layer. At the water–sediment layer interface, the boundary conditions yield

$$1 + R_{12} = T_{12} P_2^+(z=0) \tag{2}$$

$$\frac{i\gamma_1}{\rho_1}(1 - R_{12}) = \frac{T_{12}}{\rho_2}\frac{\partial P_2^+(0)}{\partial z} \tag{3}$$

where T_{ij} is the transmission coefficient at boundary ij and ρ_i and γ_i are sediment density and vertical wave number in layer i, respectively. $P_2^+(z)$ and $P_2^-(z)$ represent the down- and up-traveling fields in the sediment layer and the substitution of (2) into (3) gives

$$R_{12} = \frac{\frac{\rho_2\gamma_1}{\rho_1\gamma_2} - \frac{\partial P_2^+(0)/\partial z}{i\gamma_2 P_2^+(0)}}{\frac{\rho_2\gamma_1}{\rho_1\gamma_2} + \frac{\partial P_2^+(0)/\partial z}{i\gamma_2 P_2^+(0)}}. \tag{4}$$

Ainslie [15] defines the right terms of the denominator and numerator of (4) as

$$f^{\pm}(z) = \frac{dP_2^{\pm}/dz}{\pm i\gamma_2(z) P_2^{\pm}(z)}. \tag{5}$$

Defining ζ_{ij} as the impedance ratios $(\rho_j\gamma_i/\rho_i\gamma_j)$, (4) then becomes

$$R_{12} = \frac{\zeta_{12} - f^+(0)}{\zeta_{12} + f^+(0)}. \tag{6}$$

Considering the reflection (R_{21}) of the up-traveling signal at the water–sediment layer interface, the boundary conditions yield

$$P_2^-(0) + R_{21} P_2^+(0) = T_{21} \tag{7}$$

$$-\frac{i\gamma_1 T_{21}}{\rho_1} = \frac{1}{\rho_2}\left[\frac{\partial P_2^-(0)}{\partial z} + R_{21}\frac{\partial P_2^+(0)}{\partial z}\right]. \tag{8}$$

The substitution of (7) into (8) gives

$$R_{21} = \frac{f^-(0) - \zeta_{12}}{f^+(0) + \zeta_{12}}. \tag{9}$$

Using the similar method, R_{23} is given by

$$R_{23} = \frac{P_2^+(h)}{P_2^-(h)}\frac{f^+(h) - \zeta_{32}}{f^-(h) + \zeta_{32}}. \tag{10}$$

If the pressure field is constant with depth, $f^{\pm}(z) = 1$ and (6), (9), and (10) become reflection coefficients for layers of homogeneous fluid media.

Finally, our forward model with which to match the observed data (bottom loss) is a model for the bottom-reflection coefficient, for which the sound speed profile in the sediment layer is allowed to assume a linear k^2 profile. For this, the exact analytical and Wenzel, Kramers, and Brillouin (WKB) approximation solutions from [15] are utilized. This forward model will be governed by eight parameters, which are discussed subsequently. Note, however, that for the linear k^2 sound speed profile, a numerical error develops when the sound speed gradient is small compared to acoustic frequency. This error can be significant for the combination of high frequencies and parameters that describe low sound speed gradients. To include such gradients in the parameter space from which an optimal solution will be sought, the WKB approximation solution is used in the forward model for the field in the sediment layer instead of the exact solution when deemed necessary; otherwise, the exact solution is employed. The known WKB failure at turning points is not encountered with this protocol because turning points within the sediment layer do not arise for profiles for which this approximation is applied.

V. Inversion Based on a Two-Layered Sediment-Reflection Model

Geoacoustic parameters for the reflection coefficient model in Section IV are determined by a weighted least-squared error criterion for the total mean-squared error between a model vector based on candidate set of parameters and the data vector. Fixed values are used for the sea-water sound speed just above the sediment interface (1519 m/s) and density (1.0 g/cm^3) based on CTD measurements, while an eight-parameter set for computing the reflection coefficient is varied within ranges constrained by *a priori* information (Table I). This parameter set consists of: 1) layer thickness L; 2) sound speed at top of the sediment layer $c_2(0)$; 3) density of the sediment layer ρ_2; 4) attenuation in the sediment layer α_2/f expressed in decibels/meter/kilohertz; 5) sound speed at the bottom of the sediment layer $c_2(L)$; 6) sound speed in the half-space c_3; 7) density of the half-space ρ_3; and 8) attenuation in the half-space α_3/f. The quantity $Q = (X_i - M_i)^T W_e (X_i - M_i)$ is the objective function where, X_i is the measured bottom loss expressed in decibels, M_i is model prediction, and W_e is a diagonal weight matrix composed of $1/\sigma_n^2$ where σ_n^2 is the measurement variance for the nth bottom loss estimate (total =175). As noted previously, data variance depends somewhat on grazing angle and frequency and the objective function takes into account the data uncertainty; an

TABLE I
CONSTRAINED RANGES OF GEOACOUSTIC PARAMETERS USED FOR THE INVERSION

Parameter	Initial search space	Final search space
$c_2(0)$	1520 - 1700 (m/s)	1551 - 1562 (m/s)
$c_2(L)$	$c_2(0)$ - 2000 (m/s)	1600 - 1695 (m/s)
c_3	1550 - 2000 (m/s)	1580 - 1690 (m/s)
ρ_2	1.0 - 2.5 (g/cm^3)	1.6 - 2.3 (g/cm^3)
ρ_3	1.0 - 2.5 (g/cm^3)	1.6 - 2.3 (g/cm^3)
L	0.1 - 3.0 (m)	0.4 - 1.5 (m)
α_2/f	0.1 - 0.7 (dB/m/kHz)	0.1 - 0.4 (dB/m/kHz)
α_3/f	0.1 - 0.7 (dB/m/kHz)	0.1 - 0.4 (dB/m/kHz)

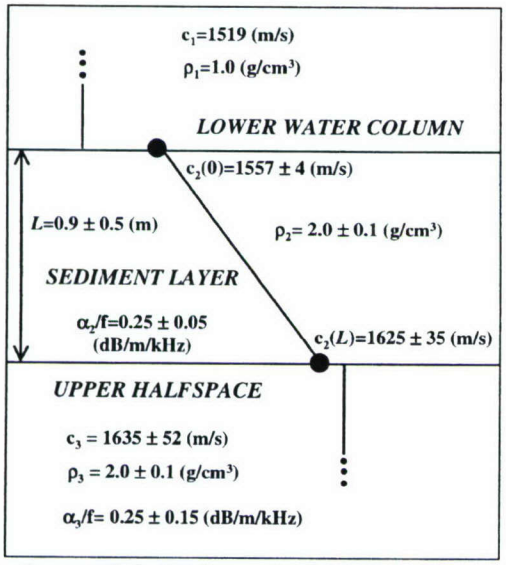

Fig. 6. Diagram of the best-fit geoacoustic parameters for two-layered sediment model and associated uncertainties.

uncorrelated error assumption is invoked insofar as constructing the W_e matrix.

There are two ranges for the parameter set shown in Table I. The larger initial search space is first examined using a coarser grid with which to discretize each parameter range. The results of this first stage of analysis readily identify a more narrowed range for each parameter, which becomes the final search space. It is this space over which an exhaustive search is completed to minimize the objective function and from which the best-fit geoacoustic parameter set is selected.

Results of the inversion for the best-fit geoacoustic parameter set describing a sediment layer and underlying sediment half-space are diagrammed in Fig. 6. Note that the best estimates for density (2.0 g/cm^3) and attenuation (0.25 dB/m/kHz) in the sediment layer and half-space are the same, which reflects, in part, an inability to resolve additional details characterizing geoacoustic parameters below the sediment layer with this mid-to-high-frequency data set. We estimate that the inversion results apply to depths no greater than about 2 m into the half-space or about 3 m into the sediment overall, given that the lowest frequency is 2 kHz, and 0.25 dB/m/kHz holds as a reasonable estimate for attenuation. The data provide little information on the sediments beyond this depth, which is the reason for the dashed line in Fig. 6.

An additional comment on attenuation is as follows: the relation between the attenuation in decibels/meter and frequency (f) can be expressed as $\alpha = bf^m$, where b is a constant and estimates of m have been reported within the range of 0.5–2 [20]. The attenuation estimated in this work, 0.25 decibels/meter/kilohertz, is by definition equivalent to a linear relation ($m = 1$) with frequency. This result should not be viewed as a contradiction of any proposed nonlinear trends, as we believe that the one-decade frequency range (2–20 kHz) in our data set is not large enough to ascertain a frequency dependence strongly different from linear. The attenuation is considered by letting the acoustic wave number in the seabed be complex. The complex wave number $\left(\tilde{k} = k(1 + i\delta)\right)$ is specified by the loss tangent δ, which is related to the attenuation coefficient according to

$$\delta(z) = \frac{bc(z)}{17.372\pi} \tag{11}$$

which implies that the loss tangent is depth dependent, but the value of $b = \alpha/f$ is a constant with depth.

The linear k^2 sound speed profile governing the reflection coefficient model is given by

$$c_2(z) = c_2(0)[1 - 2\beta z/c_2(0)]^{-1/2} \tag{12}$$

where β is the gradient of sound speed, which can be approximated by

$$c_2(z) \approx c_2(0)[1 + \beta z/c_2(0)] \tag{13}$$

for $|\beta|z/c_2(0) \ll 1$. In this result, $\beta \approx 74.77 - 0.53i$ (s^{-1}), which puts $|\beta|z/c_2(0) \approx 0.04$ at $z = L$; the reason for the quasilinear appearance in Fig. 6.

An uncertainty estimate for the eight values that compose the parameter set is made as follows. A replicate 175-point bottom-loss data set is created by randomly selecting with replacement from the original pool of bottom-loss estimates plus associated measurement variance; this is called a Bootstrap sample [17]. This sample data set is then subjected to the same objective function and evaluated over the constrained parameter search space, yielding a new parameter set called a Bootstrap replication or estimate. This process is repeated 1000 times to generate 1000 replications from which statistics can be generated. The uncertainties reported in Fig. 6 represent two standard deviations computed from these replications. Note that constraining the parameter search space can have the effect of artificially reducing estimates of uncertainty and our approach does not, as also is the case with many other inversion schemes, quantitatively address this delicate issue.

Comparisons between the measured bottom loss and the model predictions using the best-fit geoacoustic parameters are shown in Fig. 7. Over the 2–20-kHz frequency range, the measured data are in reasonable agreement with the model

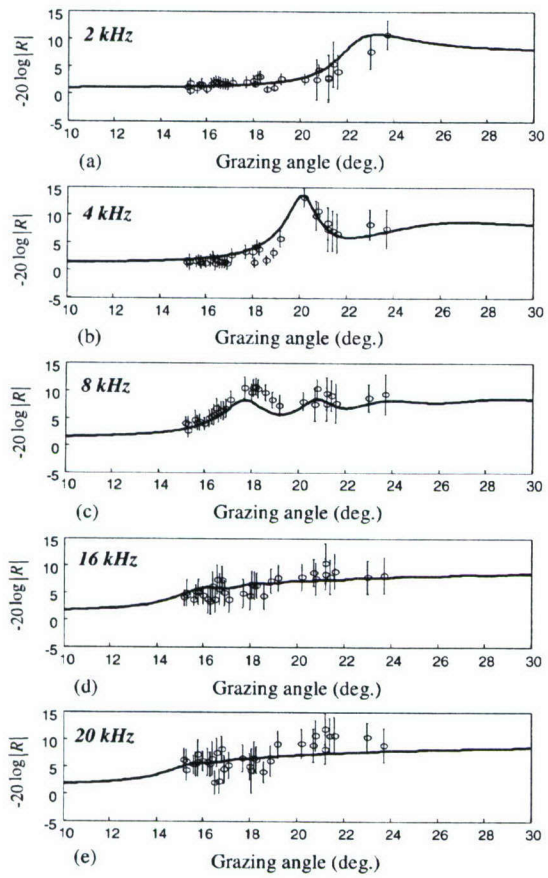

Fig. 7. Measured bottom loss as a function of grazing angle and frequency compared to model for $-20\log|R|$ based on sediment layer overlaying homogenous half-space and using the best-fit geoacoustic parameters.

predictions based on the two-layered sediment reflection coefficient model. Importantly, the significant oscillations as a function of grazing angle seen in the data at 4 and 8 kHz are captured by the model, although somewhat less so at 8 kHz. The oscillations disappear in the 2-kHz data and model, presumably because the 0.9-m sediment layer becomes nearly transparent to the 0.8-m wavelength at 2 kHz. An apparent critical angle given by $\arccos(c_1/c_3) \approx 22°$ is suggested by both the 2-kHz model and data, with this angle likely applicable to frequencies <2 kHz. Oscillations also disappear in both 16 and 20 kHz data and model; in this case, we postulate that sediment attenuation significantly reduces the sound intensity reaching the interface between the sediment layer and half-space and a much lower critical angle $\arccos\left(c_1/c_2(0)\right) \approx 13°$ appears applicable to higher frequencies.

Finally, in order to verify the assumptions concerning both plane-wave reflection and ray-based transmission loss calculations within the parameter ranges exercised by the model, we have completely duplicated our basic technique using the PE code, based on the range-dependent acoustic model (RAM; see [18]). A simulation of the received pulse in time domain is obtained via a Fourier synthesis of the narrow-band complex PE field [19]. The RAM code is run with a vertical-depth discretization of our bottom model shown in Fig. 6. For the water column,

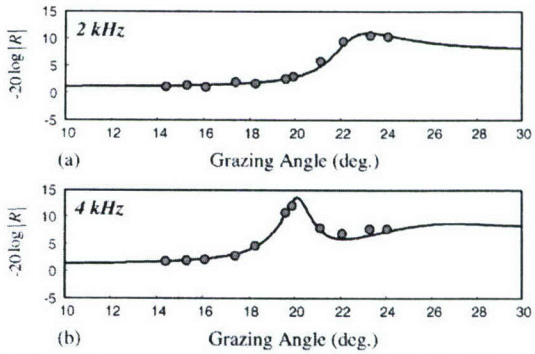

Fig. 8. Bottom loss versus grazing angle for (a) 2 and (b) 4 kHz. The solid line is the predicted value of plane wave reflection model and circles are the bottom losses obtained from time-series signals simulated using a parabolic equation (PE) code with the geoacoutic model shown in Fig. 6.

the PE is subjected to vertical-depth discretization of an average of several CTD casts. The procedure involving the PE is performed only at 2 and 4 kHz, as assumptions verified at these frequencies will hold for the higher frequencies. Results for 2 and 4 kHz are shown in Fig. 8; for both, the predicted values of plane-wave reflection model are in reasonable agreement with the bottom losses obtained from the time-domain signal calculated using the PE method. This result provides the validity for both the ray theory and the plane-wave assumption over the parameter ranges we used in this work.

VI. Summary and Conclusion

Estimates of bottom loss made within the frequency range of 2–20 kHz, and within the grazing angle range of 15°–24° have been presented and interpreted with a model for the modulus of the plane wave reflection coefficient. The measurements were made in the East China Sea, 350 km east of Shanghai in waters 105 m deep (29° 39' N, 126° 49' E) as part of the ASIAEX field program conducted in May–June 2001. The bottom-loss measurements are a subset of propagation measurements made with a source at depth 25 or 50 m and two receivers (26 and 52 m) colocated at a nominal range of 500 m. Given this measurement geometry, along with a bottom reflection rather than a bottom-scattering modality, these measurements represent an inherent horizontal average over ranges of O (10–100 m) based on the dimension of the first Fresnel zone.

Geoacoustic survey measurements [1] conducted as part of the ASIAEX field program indicated a sediment layer of O (1 m) in an area overlapping the experimental site and coring data showed a mean grain size of 3.47 ϕ, consistent with very fine sand, and a sound speed increasing from approximately 1575 m/s at the water–sediment interface to 1600–1675 m/s at approximately 1 m into the sediment. The core data in [1] also exhibit considerable vertical variation at centimeter scales or fine-scale layering. *In situ* measurements of the fine-scale bottom relief [2] put the rms bottom relief at 0.005 m (within a 4-m aperture).

Knowledge from the geoacoustic surveys motivated the construction of a forward model for the reflection coefficient based on a two-layered sediment for which the sound speed in the surficial sediment layer is allowed to vary as a linear k^2 profile and the region below this layer was modeled as

a half-space for which geoacoustic parameters are fixed. A set of eight geoacoustic parameters was identified based on a weighted least-squared error criterion between candidate parameter sets and the data, in an exhaustive search of the constrained parameter space that incorporated *a priori* information about the seabed. Estimates of uncertainty for the geoacoustic parameters were calculated using the Bootstrap method. The thickness, density, and attenuation of surficial sediment layer were estimated as 0.9 ± 0.5 m, 2.0 ± 0.1 g/cm^3, and 0.25 ± 0.05 dB/m/kHz, respectively. Sediment sound speed in the surficial layer increased from 1557 ± 4 m/s at the water–sediment interface to 1625 ± 35 m/s at depth 0.9 m. The sound speed, density, and attenuation coefficient below surficial layer (or in the half-space) were estimated as 1635 ± 52 m/s, 2.0 ± 0.1 g/cm^3, and 0.25 ± 0.15 dB/m/kHz, respectively. This parameter set produced model curves of the modulus of the plane wave reflection coefficient that agreed reasonably well with the observations of bottom loss. The parameter set also is consistent with the range of independently measured geoacoustic variables discussed in [1]. Importantly, the model curves reproduced the appearance exhibited by the data of strong variation in bottom loss as function of grazing angle at 4 and 8 kHz, combined with reduction of such variation at 2, 16, and 20 kHz. This variation in loss (reflection) with grazing angle as a function of frequency is associated with O (1 m) -thick layered structure in the near-surface sediment, which is resolvable by our mid-to-high-frequency acoustic measurements. Our inversion results apply to sediment structure at depths less than about 3 m, owing to in part the combination of lowest frequency being 2 kHz and maximum grazing angle being approximately 25°. Thus, a self-consistent construction of a geoacoustic model for this area should necessarily amalgamate the mid-to-high-frequency results given here with results obtained at lower frequencies.

ACKNOWLEDGMENT

Major instrumentation for the measurements reported here was developed by the engineering team from the Applied Physics Laboratory (APL-UW), University of Washington, Seattle, consisting of R. Light, V. Miller, P. Sabin, and J. Elliot, of which the first three, along with E. Boget (APL-UW), also helped carry out the APL-UW ASIAEX field effort. The authors thank T. Elam (APL-UW); K. B. Smith of the Naval Postgraduate School, Monterey, CA; and M. D. Collins of the Naval Research Laboratory, Washington, DC, for helpful discussions concerning time-domain implementation of parabolic equation codes. They would also like to thank the anonymous reviewers for their constructive suggestions.

REFERENCES

[1] J. H. Miller, L. R. Bartek, G. R. Potty, D. Tang, J. Na, and Y. Qi, "Sediments in the East China Sea," *IEEE J. Oceanic Eng.*, vol. 29, pp. 940–951, Oct. 2004.

[2] D. Tang, "Fine-scale measurements of sediment roughness and subbottom variability," *IEEE J. Oceanic Eng.*, vol. 29, pp. 929–939, Oct. 2004.

[3] P. H. Dahl, "Forward scattering from the sea surface and the van Cittert–Zernike theorem," *J. Acoust. Soc. Amer.*, vol. 115, pp. 589–599, 2004.

[4] ——, "On bistatic sea surface scattering: Field measurements and modeling," *J. Acoust. Soc. Amer.*, vol. 105, pp. 2155–2169, 1999.

[5] ——, "High-frequency forward scattering from the sea surface: The characteristic scales of time and angle spreading," *IEEE J. Oceanic Eng.*, vol. 26, pp. 141–151, Jan. 2001.

[6] R. E. Francois and G. R. Garrison, "Sound absorption based on ocean measurements: Part II: Boric acid contribution and equation for total absorption," *J. Acoust. Soc. Amer.*, vol. 72, pp. 1879–1890, 1982.

[7] N. P. Chotiros, "Normal incidence reflection loss from a sandy sediment," *J. Acoust. Soc. Amer.*, vol. 112, pp. 1831–1841, 2002.

[8] H. Medwin and C. S. Clay, *Fundamentals of Acoustical Oceanography*. Boston, MA: Academic, 1998.

[9] J. A. Ogilvy, *Theory of Wave Scattering from Random Rough Surfaces*. Bristol, MA: Adam Hilger, 1991.

[10] D. Tang, "Estimating shallow water bottom geo-acoustic parameters using ambient noise," in *Impact of Littoral Environmental Variability of Acoustic Predictions and Sonar Performance*, N. G. Pace and F. B. Jensen, Eds. Norwell, MA: Kluwer, 2002.

[11] C. W. Holland, "Coupled scattering and reflection measurements in shallow water," *IEEE J. Oceanic Eng.*, vol. 27, pp. 454–470, July 2002.

[12] E. L. Hamilton, "Geoacoustic modeling of the sea floor," *J. Acoust. Soc. Amer.*, vol. 68, pp. 1313–1340, 1980.

[13] A. J. Robins, "Reflection of a plane wave from a fluid layer with continuously varying density and sound speed," *J. Acoust. Soc. Amer.*, vol. 89, pp. 1686–1696, 1991.

[14] P. D. Mourad and D. R. Jackson, "High frequency sonar equation models for bottom backscatter and forward loss," in *Proc. IEEE OCEAN'89*, New York, 1989, pp. 1168–1175.

[15] M. A. Ainslie, "Reflection and transmission coefficients for layered fluid sediment overlying a uniform solid substrate," *J. Acoust. Soc. Amer.*, vol. 99, pp. 893–902, 1996.

[16] M. A. Ainslie and A. J. Robins, "Benchmark solutions of plane wave bottom reflection loss," *J. Acoust. Soc. Amer.*, vol. 104, pp. 3305–3312, 1998.

[17] B. Efron and R. Tibshirani, "Bootstrap methods for standard errors, confidence intervals, and other measures of statistical accuracy," *Stat. Sci.*, vol. 1, pp. 54–77, 1986.

[18] M. D. Collins, "A split-step Padé solution for the parabolic equation method," *J. Acoust. Soc. Amer.*, vol. 93, pp. 1736–1742, 1993.

[19] F. B. Jensen, W. A. Kuperman, M. B. Potter, and H. Schmidt, *Computational Ocean Acoustics*. New York: AIP, 1994.

[20] C. S. Clay and H. Medwin, *Acoustical Oceanography: Principles and Applications*. New York: Wiley, 1977.

Jee Woong Choi received the B.S., M.S., and Ph.D. degrees from the Department of Earth and Marine Sciences, Hanyang University, Ansan, Korea, in 1996, 1998, and 2002, respectively.

He is a Postdoctoral Research Associate with the Applied Physics Laboratory, University of Washington, Seattle.

Dr. Choi is a Member of the Acoustical Society of America and of the Acoustical Society of Korea.

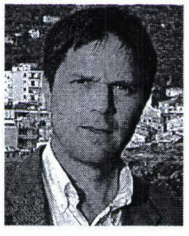

Peter H. Dahl received the Ph.D. degree in ocean engineering from the Massachusetts Institute of Technology, Cambridge/Woods Hole Oceanographic Institution, Woods Hole, MA, Joint Program in Oceanography and Oceanographic Engineering in 1989.

He currently is a Principal Engineer at the Applied Physics Laboratory, University of Washington, Seattle, where he has been since 1989, and conducts experimental and theoretical research in underwater acoustics. He also is a Research Associate Professor in the Mechanical Engineering Department, University of Washington. In 2002, he was a Guest Professor with the Department of Physics, University of Bergen, Norway.

Dr. Dahl served as an Associate Editor for the IEEE JOURNAL OF OCEANIC ENGINEERING from 1997 to 2003 and has served as Guest Editor for this Special Issue on Asian Marginal Seas. He is a Fellow of the Acoustical Society of America (ASA) and currently is Chair of the ASA Technical Committee on Underwater Acoustics. He was the U.S. Chief Scientist for ASIAEX East China Sea.